# On Similarity Solutions and Interface Reactions for a Vector-Valued Stefan Problem

**F. J. Vermolen**

Delft Institute for Applied Mathematics
Delft University of Technology
Mekelweg 4, 2628 CD Delft, the Netherlands
f.j.vermolen@tudelft.nl

**Abstract.** In this paper first it is shown for several geometries that classical similarity solutions for particle growth exist if and only if the Stefan problem is well-posed in the sense of being mass conserving. The extension of the similarity solutions to multi-component alloys, which makes the problem nonlinear, is illustrated by the application to a hypothetic alloy with realistic input values. The similarity solutions are based on the assumption of local equilibrium at the interface. In the second part, the assumption of local equilibrium is relaxed using a first-order interface reaction. The influence of the interface reaction on the movement of the interface and on the interface concentrations is evaluated using Finite Difference calculations. A Newton scheme is used to solve the nonlinear problem.

**Keywords:** particle dissolution, Stefan problem, similarity solution, diffusion, moving grid method, level-set method.

## 1   Introduction

In the thermal processing of both ferrous and non-ferrous alloys, homogenization of the as-cast microstructure by annealing at such a high temperature that unwanted precipitates are fully dissolved is required to obtain a microstructure suited to undergo heavy plastic deformation. Such a homogenization treatment is applied to hot-rolling of Al killed construction steels, HSLA steels, all engineering steels, as well as aluminum extrusion alloys. Next to precipitate dissolution, which is often the most critical of the occurring processes, particles nucleate and grow from a supersaturated solution. The minimum temperature at which the annealing should take place can be determined from thermodynamic analysis of the phases present. Another important quantity is the minimum annealing time at this annealing temperature. This time, however, is not a constant but depends on particle size, particle concentration, overall concentration, etc.

Due to the scientific and the industrial relevance of being able to predict the kinetics of particle dissolution and growth, many models of various complexity have been

presented and experimentally validated. The early models on particle dissolution and growth based on long-distance diffusion for binary alloys consisted of analytic solutions in an unbounded medium under the assumption of local equilibrium at the interface, see Ham [1, 2], Zener [3], Whelan [4], Tayler [5] (and several more references in these proceedings edited by Ockendon and Hodgkins), Howison [6] and Aaron and Kotler [7] to mention a few. The model of Nolfi et al. [8] incorporates the interfacial reaction between the dissolving particle and its surrounding phase. Part of this paper will be in the spirit of their work, but here we will consider an extension to multi-component alloys. Nolfi et al. [8] did not consider interface motion. Later modeling particle dissolution and growth has been extended to the introduction of multi-component particles by, among others, Anderson and Ågren [9], Ågren [10], Ågren and Vassilev [11], Coates [12], Bourne et al. [13], Thornton et al. [14], Reiso et al. [15], Hubert [16], Vitek et al. [17], Vusanovic and Krane [18], Atkinson et al. [19] and Vermolen et al. [20, 21]. In these papers particle dissolution and growth was viewed as a Stefan problem with a sharp interface separating the adjacent phases. Several numerical methods exist to solve Stefan problems related to particle dissolution and growth and to solidification or melting problems. A survey on numerical methods is given by Crank [22]. The most commonly used methods are the fixed grid and moving grid methods. Segal et al. [23] extended the moving grid method introduced for the Stefan problem by Murray & Landis [24] to a two-dimensional finite element framework. A state-of-the-art fixed grid method is the level set method introduced by Osher & Sethian [25]. The method was described later in a general way by Sethian [26] and by Osher & Fedkiw [27]. It was firstly applied to a Stefan problem with two spatial dimensions by Chen et al. [28]. A comparative study between the level set method, moving grid method and phase field method is due to Javierre et al. [29] and Kovačević & Šarler [30]. In a parallel study the level set method is applied for three spatial coordinates by Vermolen et al. [31] for binary alloys and by Javierre et al. [32] for multi-component alloys. Further, in the last-mentioned paper the method is extended to a vector valued Stefan problem for a multi-component alloy.

Thornton et al. [14] present an extensive review paper on the various models for precipitate dissolution and growth. In that paper, next to viewing particle dissolution and growth as a Stefan problem with a sharp interface, also diffuse-interface models, such as the phase-field method, the Cahn-Hilliard equation, are presented with the appropriate references for the metallurgical literature. Vermolen et al. [33] give a literature review on sharp-interface models for particle dissolution and growth.

In this study we describe particle growth as a Stefan problem, i.e. a diffusion equation with a moving sharp interface interface between the particle and its surrounding diffusive phase. In the first part, we assume that the particle is allowed to grow in an infinite alloy, which enables us to get exact analytic solutions for a planar, cylindrical and spherical particle. The solutions that we use here were generated by Zener [3], Coates [12], Howison [6] and Bourne et al. [13]. Subsequently, we apply the solutions to multi-component alloys, which gives a nonlinear problem to solve involving a coupled system of diffusion equations.

We note that the solutions due to Howison [6] can be applied to the growth of shape preserving ellipsoidal particles in binary alloys. Bourne et al. [13] extended these

solutions to ellipsoidal particles in multi component alloys. Furthermore, particle growth is known to give rise to a fingering behavior of the interface. This fingering behavior also occurs in two-phase flow where two adjacent immiscible phases differ in properties like density or viscocity, and this fingering is known as a so-called Saffmann-Taylor instability. An example for two phase flow in subsurface oil reservoirs is treated by, for instance, Vermolen et al. [34]. For particle growth problems in solid state alloys, this fingering was analyzed by, among many others, Mullins and Sekerka [35,36] and by Chadam et al. [37]. The interface energy, which gives rise to the Gibbs-Thomson effect, is known to stabilize the interface so that the fingering pattern disappears.

A second issue concerns the incorporation of interface reactions (such as the decomposition of chemical compounds and crossing of the interface by the atoms) into multi-component alloys. For this problem no similarity solutions exist as far as we know, and hence numerical solutions of this nonlinear problem are computed. In this paper we propose a solution method and illustrate that the influence of the interface reactions on the dissolution kinetics can be substantial.

The innovations in the present paper are the analysis of the similarity solutions and a derivation of a criterion for their existence as a solution of the Stefan problem. This has not yet been done for cylindrical and spherical particles, as far as we know. The similarity solutions that were found by Zener [3], Coates [12], Howison [6] and Bourne et al. [13], are used for this purpose. For a planar particle, this was done by Vermolen & Vuik [38]. Further, we apply a first-order interface reaction for dissolution and growth of particles in multi-component alloys, and present a numerical solution of this nonlinear problem, which is the second innovation of this paper. The similarity solutions are used as an initial guess for the numerical solution of the nonlinear problem.

## 2  The mathematical problem

The as-cast microstructure is simplified into a representative cell containing a stoichiometric $\beta$ particle with a given shape surrounded by an $\alpha$ diffusive phase in which the alloying element diffuses. The boundary between the particle and diffusive phase is referred to as the interface. Particle growth is assumed to proceed via the following steps: decomposition of the particle, crossing of the interface by the atoms from the particle and finally long-distance diffusion of the atoms in the diffusive phase. In the present paper similarity solutions are considered where long-distance diffusion is assumed to control the interface motion, i.e. local thermodynamic equilibrium is assumed at the interface and hence the interface concentration is the concentration as predicted by the thermodynamic phase diagram at the annealing temperature. Secondly, the assumption of thermodynamic equilibrium is abandoned where numerical solutions are considered for this nonlinear problem. Further, it is assumed that the particle concentration is constant all over the particle and at all stages of the dissolution process.

The interface, consisting of a point, curve or a surface for respectively a one-, two- or three-dimensional domain of computation, is denoted by $S = S(t)$. In the present similarity solutions the effects of soft-impingement are neglected, i.e. the interparticle

distance is assumed to be very large. This is an inaccurate approximation if the overall composition is large, that is, the interparticle distance is relatively small. It is known that the nucleation stage should be modeled by approaches that totally differ from the moving boundary problem until the particle reaches the size of the critical nucleus. An example of such methods is the model of (heterogeneous) nucleation and early growth due to Myhr & Grong [39], where the statistical distribution of the particle size is computed as a function of time. Further, the domain of computation is split into the diffusive part (the $\alpha$-diffusive phase), denoted by $\Omega = \{x \in \mathbb{R} : x > S(t)\}$ and the $\beta$-particle $\Omega_p = \{x \in \mathbb{R} : 0 < x < S(t)\}$. First, the binary problem is posed. Subsequently the multi-component model is described. This is done for both thermodynamic equilibrium and non equilibrium.

## 2.1 The binary model

The distribution of the alloying element is determined by diffusion in the diffusive phase $\Omega$, which gives

$$\frac{\partial c}{\partial t} = D\Delta c = D\left\{\frac{\partial^2 c}{\partial r^2} + \frac{a}{r}\frac{\partial c}{\partial r}\right\}, \quad \text{for } r \in \Omega \text{ and } t > 0. \tag{1}$$

Here $D$ represents the diffusion coefficient and $r$ denotes the spatial position within the domain of computation. Further, $a = 0$, $a = 1$, $a = 2$ respectively correspond to planar, cylindrical and spherical symmetry. In the present study $D$ is treated as a constant. Within the particle the concentration is equal to a given constant, hence

$$c = c^{\text{part}}, \quad \text{for } r \in \Omega_p \text{ and } t \geq 0. \tag{2}$$

On the interface, $S(t)$, local equilibrium is assumed, that is. The concentration is as predicted by the thermodynamic phase diagram, i.e.

$$\lim_{r \to S^+(t)} c = c^{\text{sol}}, \quad \text{for } t > 0. \tag{3}$$

The initial concentration is denoted by $c^0$. Further, it is assumed that the concentration did not change at infinity, hence

$$\lim_{r \to \infty} c = c^0, \quad \text{for } t > 0. \tag{4}$$

Since the concentration satisfies a maximum principle, the above relation implies a horizontal asymptote at infinity. From a mass balance, the equation of motion of the interface can be derived, this equation is commonly referred to as the Stefan condition, and is given by:

$$(c^{\text{part}} - c^{\text{sol}})S'(t) = D \lim_{r \to S^+(t)} \frac{\partial c}{\partial r}, \quad \text{for } t > 0. \tag{5}$$

Here $S'(t)$ represents the interface velocity. The problem is completed with the initial position of the interface $S(0) = 0$, i.e. there is no particle initially. The problem, consisting of equations (1), (2), (3), (4) and (5), is referred to as a Stefan problem for particle

dissolution or particle growth. We also remark that the Stefan problem is well-posed in the sense of mass conservation if and only if $c^0 \in (\min\{c^{\mathrm{sol}}, c^{\mathrm{part}}\}, \max\{c^{\mathrm{sol}}, c^{\mathrm{part}}\})$. This result was proved in [38] for an unbounded domain and [40] for a bounded domain.

For the above presented problem Zener-type analytic solutions for various geometries can be obtained using the Boltzmann transformation.

## 2.2 The multi-component model

In this section the same definitions for geometry as in the previous section are used. However, now the simultaneous diffusion of several alloying elements and the interaction from cross-diffusion are considered. Let $n_S$ be the total number of chemical elements that are considered, then we have for each alloying element $i$:

$$\frac{\partial c_i}{\partial t} = \sum_{j=1}^{n_S} D_{ij} \Delta c_j = \sum_{j=1}^{n_S} D_{ij} \left\{ \frac{\partial^2 c_j}{\partial r^2} + \frac{a}{r} \frac{\partial c_j}{\partial r} \right\}, \quad \text{for } r \in \Omega \text{ and } t > 0. \tag{6}$$

The above equation with cross-diffusion creates a set of strongly coupled equations, where $D_{ij}$ represents the influence of species $j$ on the rate of diffusion of species $i$. The particle concentration is treated as a constant as before, i.e. for each chemical element $i$:

$$c_i = c_i^{\mathrm{part}}, \quad \text{for } r \in \Omega_p \text{ and } t \geq 0. \tag{7}$$

On the interface, local equilibrium is assumed, hence the interface concentrations are determined by the phase diagram following from thermodynamics, that is

$$F(c_1^S, \ldots, c_{n_S}^S) = 0, \tag{8}$$

where $c_i^S := \lim_{r \to S^+(t)} c_i$. In general, this equation poses an essential nonlinearity. In the ideal stoichiometric case, the above relation is hyperbolic, resulting into

$$(c_1^S)^{m_1}(\ldots)(c_{n_S}^S)^{m_{n_S}} = K. \tag{9}$$

To keep things general, the above function $F$ is assumed to be known. Similarly as in the binary model, the initial concentration is known and denoted by $c_i^0$ for all chemical elements, and hence at infinity we have for each chemical element $i$:

$$\lim_{r \to \infty} c_i = c_i^0, \quad \text{for } t > 0. \tag{10}$$

From a mass balance, the equation of motion of the interface can be derived, therewith we get for each alloying element $i$:

$$(c_i^{\mathrm{part}} - c_i^S)S'(t) = \lim_{r \to S^+(t)} \sum_{j=1}^{n_S} D_{ij} \frac{\partial c_j}{\partial r}, \quad \text{for } t > 0. \tag{11}$$

From the above set of equations, the interface concentrations, concentration profiles in $\Omega$ and interface velocity and position are obtained. Note that the interface concentrations $c_i^S$

have to be determined as part of the solution. First, the interface velocity can be eliminated since the above equation (11) has to hold for each alloying element. This gives

$$\frac{1}{c_i^{\text{part}} - c_i^S} \lim_{r \to S^+(t)} \sum_{j=1}^{n_S} D_{ij} \frac{\partial c_j}{\partial r} = \frac{1}{c_k^{\text{part}} - c_k^S} \lim_{r \to S^+(t)} \sum_{j=1}^{n_S} D_{kj} \frac{\partial c_j}{\partial r}, \tag{12}$$

for each $i \neq k$, for $t > 0$.

The concentrations at the interface, $c_i^S$, satisfy the above equation and equation (8). Equations (8) and (12) make the problem nonlinear. We remark that the well-known tie line construction defines the final equilibrium concentrations on the relation (8). Setting the diffusion coefficients equal gives these equilibrium concentrations as well. Further, the tie lines can be used to predict the final equilibrium particle size in the case of a bounded domain of computation. This all does not play a role here, hence the tie line construction is not used. The above problem is solved in Section 3.3.

The unknowns in the problem as constituted by equations (8)–(12) are the interface position $S(t)$, interface concentrations $c_i^S$ and concentration profiles $c_i(r, t)$. To determine the interface position, it is necessary to compute $c_i(r, t)$ and hence also $c_i^S$. To determine $c_i^S$ one solves the nonlinear equations resulting from equations (10), (11) and (12). In the first part analytic solutions are obtained for $c_i(r, t)$, which are substituted into expression (12) and (11) to obtain a nonlinear equation for the interface concentration from which the interface position is computed. In the second part of the paper, numerical solutions are addressed for the case of interface reactions. The incorporation of interface reactions is described in the next section.

### 2.2.1 The interface reaction for the vector-Stefan problem

As mentioned in the previous section, equations (10), (11) hold for local thermodynamic equilibrium, that is, the interface concentrations directly follow from the phase diagram. Physically, multi-component particle dissolution takes place by the following consecutive steps: 1. decomposition of the chemical compound; 2. crossing of the interface by the atoms; and 3. long-distance diffusion through the diffusive phase. Particle growth takes place by the reverse of the above-mentioned steps. In classical particle dissolution/growth models, diffusion is assumed to be the rate-determining step. In the solution of the second part of the paper, this assumption is relaxed. The flow of atoms out of or into the particle is assumed to satisfy a first order reaction, that is, $K_{\text{int},i}(c_i^S - c_i(S(t), t))$ for each species $i$. This must be balanced by the diffusion of the species $i$ into or out of the diffusive phase and by the displacement of the interface $S(t)$: $\sum_{j=1}^{n_S} D_{ij} \frac{\partial c_j}{\partial r}(S(t), t) + c_i(S(t), t)S'(t)$. This results into the following Robin condition at the interface

$$K_{\text{int},i}\big(c_i^{\text{sol}} - c_i(S(t), t)\big) = \sum_{j=1}^{n_S} D_{ij} \frac{\partial c_j}{\partial r} + c_i(S(t), t)S'(t). \tag{13}$$

The above equation holds for all chemical species $i$. The above equation is derived analogously to the case that the off-diagonal diffusion coefficients are zero. The equation

of motion becomes

$$\left(c_i^{\text{part}} - c_i(S(t), t)\right) S'(t) = \sum_{j=1}^{n_S} D_{ij} \lim_{r \to S^+(t)} \frac{\partial c_j}{\partial r}, \quad \text{for } t > 0. \tag{14}$$

We note that the equilibrium concentrations $c_i^S$ satisfy the nonlinear relation (10), (11). The interface concentrations $c_i(S(t), t)$ satisfy the above relation (14). As far as we know, no analytic solutions in terms of similarity solutions exist for the problem with interface reactions. Therefore, we present our preliminary numerical solutions for particle dissolution/growth with the incorporation of interface reactions. The idea is to incorporate our approach into our three-dimensional code for particle dissolution in multi-component alloys.

## 3   Analytic solutions

First the analytic solutions for the binary case, which are the backbone for the multi-component case, are reviewed briefly. Subsequently, conditions for the existence of these analytic solutions are analyzed and subsequently some examples are given of the extension to multi-component alloys. We note here that the self similar solutions were derived in many earlier studies, due to Howison [6], Tayler [5], Atkinson [19], Bourne et al. [13], Ham [1, 2, 41] and Zener [3], and the list is far from complete. For the sake of completeness, first we repeat the most important steps.

### 3.1   Solutions for the binary model

As an *ansatz* solutions in the form of $c(r, t) = u(\eta)$, where $\eta := \frac{r}{\sqrt{t}}$ and $S(t) = k\sqrt{t}$, were obtained as similarity solutions due to Zener.

After some elementary algebra and use of the boundary conditions, which are

$$\lim_{\eta \to k^+} u = c^{\text{sol}}, \quad \text{and} \quad \lim_{\eta \to \infty} u = c^0, \tag{15}$$

one obtains for the concentration for $x > k$:

$$u(\eta) = \frac{c^0 - c^{\text{sol}}}{\int_k^\infty \frac{1}{z^a} \exp\left(-\frac{z^2}{4D}\right) dz} \int_k^\eta \frac{1}{z^a} \exp\left(-\frac{z^2}{4D}\right) dz + c^{\text{sol}}. \tag{16}$$

The equation of motion (5) is used to determine the value of $k$

$$\frac{dS}{dt} = \frac{k}{2\sqrt{t}} = \frac{D}{c^{\text{part}} - c^{\text{sol}}} \frac{u'(k)}{\sqrt{t}}. \tag{17}$$

Differentiation of equation (31) and substitution of the result into equation (17) gives the following transcendental equation for $k$

$$\frac{k}{2} = \frac{D}{c^{\text{part}} - c^{\text{sol}}} \cdot \frac{c^0 - c^{\text{sol}}}{\int_k^\infty \frac{1}{z^a} \exp\left(-\frac{z^2}{4D}\right) dz} \cdot \frac{\exp\left(-\frac{k^2}{4D}\right)}{k^a}. \tag{18}$$

In the above expression the integral has to be evaluated for the various values of $a$, that is for the various geometries. Therefore, the integral $I_a$ is defined by

$$I_a := \int_k^\infty \frac{1}{z^a} \exp\left(-\frac{z^2}{4D}\right) dz. \tag{19}$$

First, by substitution of $y := \frac{x}{2\sqrt{D}}$, one obtains

$$I_a = \frac{1}{(2\sqrt{D})^{a-1}} \int_{\frac{k}{2\sqrt{D}}}^\infty \frac{\exp\left(-y^2\right)}{y^a} dy. \tag{20}$$

Now the cases $a = 0$, $a = 1$ and $a = 2$ are treated consecutively. For $a = 0$, which is the planar particle, this gives

$$I_0 = 2\sqrt{D} \int_{\frac{k}{2\sqrt{D}}}^\infty \exp\left(-y^2\right) dy = \sqrt{\pi D}\, \mathrm{erfc}\left(\frac{k}{2\sqrt{D}}\right), \tag{21}$$

which is the familiar result for particle growth. For $a = 1$, which is the cylindrical particle, one obtains

$$I_1 = \int_{\frac{k}{2\sqrt{D}}}^\infty \frac{\exp\left(-y^2\right)}{y} dy = \frac{1}{2} \int_{\frac{k^2}{4D}}^\infty \frac{\exp\left(-u\right)}{u} du = \frac{1}{2} Ei\left(\frac{k^2}{4D}\right), \tag{22}$$

which is the exponential integral. Finally for $a = 2$, which is the spherical particle, this yields

$$I_2 = \frac{1}{2\sqrt{D}} \int_{\frac{k}{2\sqrt{D}}}^\infty \frac{\exp\left(-y^2\right)}{y^2} dy = \frac{\exp\left(-\frac{k^2}{4D}\right)}{k} - \frac{1}{2}\sqrt{\frac{\pi}{D}}\, \mathrm{erfc}\left(\frac{k}{2\sqrt{D}}\right). \tag{23}$$

These expressions (21), (22) and (23) are substituted into equation (18) and, then a solution for the interface velocity parameter $k$ is obtained after a zero-point method. The above integrals can be classified as gamma-functions. The solutions that have been derived here are the classical Zener solutions. We will analyze the existence of a solution.

## 3.2 Existence of similarity solutions

For convenience, first the nonlinear problem to be solved will be re-written in terms of the independent variable $x := \frac{k}{2\sqrt{D}}$ and $A := \frac{c^0 - c^{\mathrm{sol}}}{c^{\mathrm{part}} - c^{\mathrm{sol}}}$, which gives

$$\frac{x}{A} = \frac{\exp\left(-x^2\right)}{2x^a \int_x^\infty \frac{\exp\left(-y^2\right)}{y^a} dy} =: f(x; a). \tag{24}$$

To obtain the solution of the Stefan problem, the above relation has to be solved to obtain $x$. Note, that since we consider particle growth, that we are only interested in non-negative solutions $x$. Graphically, we need to determine the intersection of the functions at the left- and right hand side of the above equation (see Fig. 1). Subsequently, the interface speed number $k$ can be obtained by using $k = 2\sqrt{D}x$. This problem is solved using a zero-point method. Further, we remark that the improper integral $I_a$ over the interval $(0, \infty)$ only exists if $a = 0$, that is

$$\int_0^\infty \frac{\exp(-y^2)}{y^a} dy = \begin{cases} \frac{\sqrt{\pi}}{2}, & \text{if } a = 0, \\ \text{does not exist}, & \text{if } a \in \{1, 2\}. \end{cases} \tag{25}$$

Further,

$$\lim_{x \to 0^+} f(x; a) = \begin{cases} 1, & \text{if } a = 0, \\ \text{does not exist}, & \text{if } a \in \{1, 2\}. \end{cases} \tag{26}$$

It is observed that $f(x; a)$ is concave-upward on $x > 0$ for $a \in \{0, 1, 2\}$ and that

$$\lim_{x \to \infty} \frac{f(x; a)}{x} = 1, \tag{27}$$

for $a \in \{1, 2, 3\}$. We also note that $f(x; a) > 0$ strictly. Further it is observed that $f(x; 0) < f(x; 1) < f(x; 2)$ for $x > 0$. For $a = 0$ it is trivial to see that $f(0; 0) = 1$. In the cases that $a \in \{1, 2\}$, we have that for each $L > 0$ there exists a $\delta > 0$ such that $0 < x < \delta \Rightarrow f(x; a) > L$. Since $\lim_{x \to \infty} \frac{f(x; a)}{x} = 1$, there is a point of intersection between $f(x; a)$ and $x/A$ for $x \geq 0$ if and only if $0 < A < 1$.
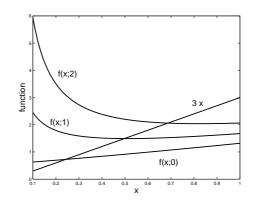


Fig. 1. The function $f(x; a)$ for various values of $a$ and $\frac{x}{A}$ as a function of $x$. From the bottom to the top the curves correspond to $a = 0, 1, 2$. The intersection points are the solution of the Stefan problem.

This implies that $c^0$ must be between $c^{\text{sol}}$ and $c^{\text{part}}$ for a similarity solution to exist. This is in agreement with the criterion for well-posed solutions in the sense that these solutions are mass conserving. Hence, we proved the following assertion:

**Theorem 1.** *Consider the Stefan problem as constituted by equations* (1)–(5) *with $A > 0$ (the particle* growth *case). Then,*

- *The initial concentration satisfies $c^0 \in (\min\{c^{\text{sol}}, c^{\text{part}}\}, \max\{c^{\text{sol}}, c^{\text{part}}\})$ iff the Stefan problem is well-posed (see Theorem* 1 *in Vermolen et al.* [33]*).*

- *The Stefan problem for the unbounded domain is well-posed iff there exists a similarity solution in the form $c = c(r/\sqrt{t})$ and $S(t) = k\sqrt{t}$ for the* **growth** *problem, i.e. $A > 0$ of planar, cylindrical and spherical particles (i.e. $a = 0, 1, 2$).*

In [38] and [40] the assertion has been proved for unbounded and general dimensional bounded domains respectively, that there exists a mass conserving solution for the particle growth problem if $0 < A < 1$. In the present work, it is demonstrated for the particle growth problem in an unbounded domain that a similarity solution exists if and only if $0 < A < 1$, which is exactly the same condition needed for the existence of a mass conserving solution.

For the unbounded case the similarity solution to the Stefan problem for the particle growth problem as in equations (1)–(5) is unique if the above condition is satisfied. The claim of uniqueness among the class of similarity solutions is sustained by the following argument: Suppose that a similarity solution exists and suppose that it is not unique. Then $f(x; a)$ has more than one intersection with the line $y = \frac{x}{A}$. Since,

$$\lim_{x \to \infty} \frac{f(x; a)}{x} = 1,$$

it follows that $\lim_{x \to \infty} f'(x; a) = 1 < \frac{1}{A}$ for $0 < A < 1$. This implies that if the intersection of $f(x; a)$ with $\frac{x}{A}$ is not unique, then $f(x; a)$ is no longer concave-upward on $x > 0$. This contradicts the observation that $f(x; a)$ is concave-upward for $x > 0$ for $a \in \{0, 1, 2\}$, and hence the similarity solution is unique if $0 < A < 1$.

For the sake of illustration, we plot the functions $x/A$ and $f(x; a)$ for $a \in \{0, 1, 2\}$ in Fig. 1 for $A = 1/3$. It can be seen that the particle growth velocities are ordered from low to high: planar – cylindrical – spherical. This can be understood by $0 < f(x; 0) < f(x; 1) < f(x; 2)$ for $x > 0$ and the limit $\lim_{x \to \infty} \frac{f(x; a)}{x} = 1$ for $a \in \{0, 1, 2\}$. The result that we demonstrated here is needed to investigate the validity of numerical solutions for the multi-component setting.

### 3.3 Similarity solutions for the multi-component model

For completeness we repeat some of the principles outlined in Vermolen & Vuik [21]. First it is observed that the multi-component Stefan problem can be written in vector form:

$$\frac{\partial \underline{c}}{\partial t} = D\Delta \underline{c}, \tag{28}$$

where $D$ represents the diffusion matrix. Further, for the equation of motion, we have

$$(\underline{c}^p - \underline{c}^s)v_n = D\frac{\partial \underline{c}}{\partial n} \tag{29}$$

on the moving interface, where $v_n$ and $\frac{\partial c}{\partial n}$ respectively denote the interface velocity and directional derivative in the outward normal. As in [21] we diagonalize $D$ (or use a Jordan form if the matrix is not diagonalizable), to obtain $D = P\Lambda P^{-1}$, where $P$ has the eigenvectors of $D$ as its columns and $\Lambda = \mathrm{diag}(\lambda_1 \ldots \lambda_{n_S})$, with $\lambda_i$ as the eigenvalues of $D$. Now the strong coupling in the diffusion equations has been removed and the diffusion equations and the equation of motion can be rewritten by

$$
\begin{aligned}
\frac{\partial \underline{u}}{\partial t} &= \Lambda \Delta \underline{u}, \\
(\underline{u}^p - \underline{u}^s)v_n &= D\frac{\partial \underline{u}}{\partial n}.
\end{aligned}
\tag{30}
$$

Note that $\underline{c} = P\underline{u}$ and equation (8) has to be adjusted to have an expression in $\underline{u}^S$.

The similarity solution is analogous to the one in Section 3.1, but now for all chemical species $i \in \{1, \ldots, n_S\}$:

$$
u_i(\eta) = \frac{u_i^0 - u_i^{\mathrm{sol}}}{\int_k^\infty \frac{1}{z^a} \exp\left(-\frac{z^2}{4\lambda_i}\right)dz} \int_k^\eta \frac{1}{z^a} \exp\left(-\frac{z^2}{4\lambda_i}\right)dz + u_i^{\mathrm{sol}}.
\tag{31}
$$

As before, we obtain for the interface motion with the concentration profiles for all chemical species $i \in \{1, \ldots, n_S\}$:

$$
\frac{k}{2} = \frac{\lambda_i}{u_i^{\mathrm{part}} - u_i^S} \cdot \frac{u_i^0 - u_i^S}{\int_k^\infty \frac{1}{z^a} \exp\left(-\frac{z^2}{4\lambda_i}\right)dz} \cdot \frac{\exp\left(-\frac{k^2}{4\lambda_i}\right)}{k^a}.
\tag{32}
$$

Next to the above equation, equation (8) holds. Hence equations (8) and (32) constitute a system of nonlinear algebraic equations to be solved for $c_i^S$ and interface velocity parameter $k$. Note that for $a = 0$ the planar solution as in [42] is retrieved. Note further that equations (21), (22) and (23) can be substituted into the integral in the above equation to be solved by a zero-point method for a system of algebraic equations. We note that the above expression is similar to the one in Bourne et al. [13] and Coates [12], although its derivation is different here. The results of this section are used to validate numerical solutions and to have an initial guess for the interface concentrations which have to be obtained from numerical solution of the nonlinearly coupled problem.

### 3.4 Examples of calculations with the similarity solutions

In the simulations of this section, we set the off-diagonal diffusion coefficients equal to zero and we set for convenience $D_{ii} =: D_i$.

### 3.4.1 *The influence of the ratio $\frac{D_1}{D_2}$*

As a basic configuration a hypothetic case with

$$
c_1^{\mathrm{part}} = 50 = c_2^{\mathrm{part}}, \quad c_1^0 = 2 = c_2^0, \quad D_1 = 1, \quad c_1^S c_2^S = K = 1,
\tag{33}
$$

is dealt with, though the numbers have the same order of magnitude as aluminum alloys under the conditions of a heat treatment. Here the diffusion coefficient of the second alloying element is varied for the several geometries. The results have been plotted in Fig. 1 where $k$ is displayed as a function of $D_2$ for the three geometries. From Fig. 2 it is clear that also in the multi-component case the spherical particles grow fastest and that the planar particle are the slowest. Further, from Fig. 2 it can be seen that for $D_2 \rightarrow 0$ and $D_2 \rightarrow \infty$ the derivative of the dissolution speed with respect to $D_2$ becomes smaller. This holds for all cases.
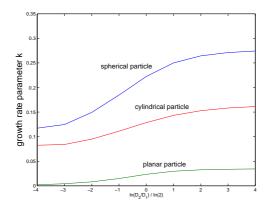


Fig. 2. The growth rate parameter $k$ as a function of the logarithm of the ratio of the diffusivities for a spherical, cylindrical and spherical particle.

## 4  Numerical solutions for multi-component simulations with an interface reaction

### 4.1  The numerical procedure

In the numerical literature there is a vast jungle of methods to solve Stefan problems and moving boundary problems. Among many other methods, such as variational inequalities and the enthalpy method, the level-set method, phase-field method and the moving grid method are the most popular ones. The level-set method was introduced by Osher and Sethian [25] and was applied for the first time to a Stefan problem by Chen et al. [28]. Nowadays, we are applying the level-set method to Stefan problems in three spatial dimensions in some other studies [33] and [32] for both binary and multi-component alloys.

For some metallic systems, especially with strongly stable, complicated chemical compounds (with a very high activation energy to decompose), the interface reactions proceed slowly in relation to long-distance diffusion. This implies that a Robin condition at the interface is to be used. In this section we propose a numerical method to deal with this issue and this method will be implemented into our computer code for multi-component particle dissolution in three spatial dimensions. In this paper the calculations

with the interface reaction for a vector-Stefan problem have been done by the use of the moving grid method. The moving grid method for a Stefan problem was introduced by Murray and Landis [24] for one spatial dimension. It was extended in a finite element framework for our class of Stefan problems by Segal et al. [23]. The extension involved a conservative discretization at the moving boundary for initially non-smooth interfaces, such as disk-like particles.

More details about the presently used numerical scheme for the multi-component problem can be found in [33] in Section 3.2.1. The only addition to the numerical scheme in the present paper is the Robin boundary condition from the interface reaction, which is discretized by

$$K_{\text{int},i}(c_i^{\text{sol}} - c_{i,0}) = \sum_{j=1}^{n_S} D_{ij} \frac{-3c_{j,0} + 4c_{j,1} - c_{j,2}}{2\Delta r} + c_{i,0} S'(t), \tag{34}$$

where $c_{j,k}$ denotes the concentration of the $j$-th species on the $k$-th gridnode ($c_{j,0}$ hence denotes the interface concentration of species $j$). To obtain the interface velocity, we do not discretize the equation of motion equation (14) but we substract equation (14) from the Robin boundary condition, to obtain

$$S'(t) = \frac{K_{\text{int},i}}{c_i^{\text{part}}}(c_i^{\text{sol}} - c_{i,0}). \tag{35}$$

Here we do not have the trouble of computing a numerical approximation of the gradient of the concentration after having obtained the concentration profile. Note that the interface velocity must be the same for all chemical species, hence

$$\frac{K_{\text{int},i}}{c_i^{\text{part}}}(c_i^{\text{sol}} - c_{i,0}) = \frac{K_{\text{int},k}}{c_k^{\text{part}}}(c_k^{\text{sol}} - c_{k,0}), \tag{36}$$

where $i \neq k$. Further the nonlinear equation (8) has to hold. Equations (34), (8), (36) pose a sufficient number of equations to determine the unknown values $c_i^{\text{sol}}$ and $c_{i,0}$ for $i \in \{1, \ldots, n_S\}$. The interface position is subsequently determined by equation (35).

The problem is nonlinear due to equation (8). Several methods, like Broyden's method, Picard's fixed point method and a Newton scheme with finite differences for the entries of the Jacobian matrix (referred to as the "quasi-Newton method") can be used. In this study we compared Picard's method with the quasi-Newton scheme. The quasi-Newton scheme appeared to be more efficient and therefore the description of the numerical method to solve the equations will be devoted to this method. For illustrative purposes we present the description for two species, that is $n_S = 2$.

At each time step we carry out an iterative procedure to obtain $c_1^S$ and $c_2^S$ and the interface position, $S$, at $t^{n+1}$. The interface concentrations $c_{1,0}$ and $c_{2,0}$ follow from the solution of the diffusion equations with the Robin boundary condition. We have to solve the following set of equations:

$$f_1(c_1^S, c_2^S, c_{1,0}, c_{2,0}) = \frac{K_{\text{int},1}}{c_1^{\text{part}}}(c_1^S - c_{1,0}) - \frac{K_{\text{int},2}}{c_2^{\text{part}}}(c_2^S - c_{2,0}) = 0,$$
$$f_2(c_1^S, c_2^S, c_{1,0}, c_{2,0}) = (c_1^S)^{m_1}(c_2^S)^{m_2} - K = 0. \tag{37}$$

The above set of equations is solved by Newton's method, where at each step the concentration profile on the entire domain of computation is required, with the use of the boundary conditions at the interface

$$
\begin{aligned}
K_{\text{int}_1}(c_1^S - c_{1,0}) &= \sum_{j=1}^{n_S} D_{1j} \frac{-3c_{j,0} + 4c_{j,1} - c_{j,2}}{2\Delta r} + c_{1,0}S'(t), \\
K_{\text{int}_2}(c_2^S - c_{2,0}) &= \sum_{j=1}^{n_S} D_{2j} \frac{-3c_{j,0} + 4c_{j,1} - c_{j,2}}{2\Delta r} + c_{2,0}S'(t),
\end{aligned}
\tag{38}
$$

by which $c_{1,0}$ and $c_{2,0}$ are determined. We note that at a boundary not being a moving interface, a homogeneous Neumann condition is imposed. We must bear in mind that the interfacial position $S(t^{n+1})$ and interface velocity $S'(t^{n+1})$ are also required using expression (35). Therefore, coinciding with each Newton iteration-step, the interface position is updated using expression . This gives an array of $c_{1,0}$, $c_{2,0}$, $c_1^S$, $c_2^S$ and $S(t^{n+1})$ at the new time-step $t^{n+1}$. At each Newton step, $p$, the interface position is updated according to

$$
S_p(t^{n+1}) = S(t^n) + \frac{\Delta t}{2}\left\{ S'(t^n) + S_p'(t^{n+1}) \right\},
\tag{39}
$$

where $S_p'(t^{n+1})$ is computed with $c_{1,0}$, $c_{2,0}$, $c_1^S$ and $c_2^S$ and the corresponding concentration profiles $c_1(r,t)$ and $c_2(r,t)$ (computed with these numbers) at each iteration step. Let $\underline{x}^p := (c_{1,p}^{S,n+1}, c_{2,p}^{S,n+1})^T$, where $p$ denotes the iteration number, then, the complete algorithm can be summarized by

```
Enter initial concentration profile
Enter initial interface position
t = 0, n = 0
do until t > t_end
   t = t + Δt
   x¹ = (c_{1,p}^{S,n}, c_{2,p}^{S,n})^T
   p = 1
   do until convergence
     Solve concentration profiles for x^p
     Compute the entries of the Jacobian by finite
     differences
     x^{p+1} = x^p - J^{-1}(x^p)f(x^p)
     p = p + 1
     S_p(t^{n+1}) = S(t^n) + Δt/2 {S'(t^n) + S_p'(t^{n+1})}
   end do
```

$$S(t^{n+1}) = S_p(t^{n+1})$$
$$n = n + 1$$

```
end do
```

This formulation allows a straightforward application to $n_S$ species. As initial estimate for the concentrations $c_1^S$ and $c_2^S$ we use the results from the similarity solutions for local equilibrium as described in the previous part. Note that for the case of particle growth one can use the similarity solution for each geometry. However, for particle dissolution, we only have a similarity solution for the planar case. Then, this is the only possibility to use as initial values for $c_1^S$ and $c_2^S$.

Since the interface concentrations $c_{1,0}$ and $c_{2,0}$, for each value of $c_1^S$ and $c_2^S$, for each value of $c_1^S$ and $c_2^S$ the complete concentration profiles must be computed. Hence a major disadvantage of the Newton method is the need of the numerical computation of the Jacobian entries. So at each Newton step we need three evaluations of the concentration profiles. Whereas the fixed point algorithm just requires one evaluation of the concentration profiles at each step. On the other hand, Newton converges quadratically and Picard's fixed point algorithm converges linearly if the object function is a contraction. Picard's scheme could be accelerated by choosing an appropriate relaxation parameter $\delta$ in

$$\underline{x}^{p+1} = \underline{x}^p - \delta \underline{f}(\underline{x}^p), \text{ where } \underline{f}(\underline{x}) = \left( f_1(\underline{x}), f_2(\underline{x}) \right)^T. \tag{40}$$

At the first time-step Picard's scheme typically required more than 40 iterations to reach the same an error. As time proceeds the number of iterations decreases for both methods, and the difference of the required number of iterations decreases. For the simulation, shown in Fig. 3 and 4 for $K_{\text{int},1} = 1$ and $K_{\text{int},2} = 1$ the ratio between the computation times for both methods was 0.88. For a three dimensional implementation of this problem, Picard may be an interesting alternative, since the numerical determination of the Jacobian will become very expensive then. This will be studied in a future study.

### 4.2 Numerical results

To illustrate the influence of the interface reaction rate parameter, we consider a plate-like particle with initial size of 0.1 $\mu m$ which dissolves in a computational cell of 1 $\mu m$. We consider two chemical species with diffusion coefficients $D_{11} = 1\mu m^2/s$, $D_{22} = 2\mu m^2/s$, $D_{12} = 0 = D_{21}$. The solubility product is chosen to one, that is

$$c_1^S c_2^S = 1. \tag{41}$$

The interface reaction rate parameters $K_{\text{int},1}$ and $K_{\text{int},2}$ are taken equal and values have been assigned of 1, 10, 100 and infinite. As to be expected the value of 100 is very close to the local equilibrium solutions as the limit case $K_{\text{int},1}$ and $K_{\text{int},2} \to \infty$ in which $c_i(S(t), t) = c_i^S$. In Fig. 3 it can be seen clearly that lower values of the interface reaction rate parameter delay the dissolution process considerably. Physically, this means that the reactions at the interface, which are the decomposition of the chemical compounds in the particle and the subsequent crossing of the interface by the atoms, are so slow that the

atoms are not supplied sufficiently fast to match with the depletion of the atoms from the interface by long-distance diffusion. From Fig. 3 it can be seen that interface controlled dissolution is far more sluggish than diffusion controlled dissolution. In Fig. 4 it can be seen that the interface reaction parameter also influences the solid solubilities and the interface concentrations. This gives smaller concentration gradients for the cases of low values of $K_{\mathrm{int,i}}$. Hence the dissolution speed is lowered.
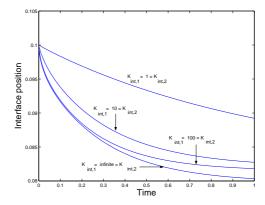


Fig. 3. The interface position as a function of time for various values of the interface reaction parameters $K_{\mathrm{int,1}}$ and $K_{\mathrm{int,1}}$.
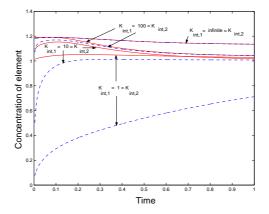


Fig. 4. The interface concentrations and solubilities of the first element as a function of time for various values of the interface reaction parameters $K_{\mathrm{int,1}}$ and $K_{\mathrm{int,1}}$. The solid lines indicate the solubility of the first chemical element and the dashed lines correspond to the interface concentrations.

## 5   Discussion and conclusions

Since metallic alloys often contain secondary particles in the form of plates, needles and spherical particles, analytic solutions for several geometries have been constructed for

the growth of particles. These particles grow as a result from nucleation and diffusion. The earliest nucleation stage proceeds by steps that cannot be dealt with by the present model since the particle has to grow larger than a critical nucleus size due to the surface tension effects. This process is modeled in the nucleation models, such as the (heterogeneous) model due to Myhr and Grong [39], in the Avrami-style models, or in the spirit of Monte-Carlo simulations. The present similarity solutions neglect this behavior and are constructed as a mathematical exercise that can be used to calibrate the results of numerical models for the case that the Gibbs-Thomson effect and nucleation issues have been disregarded. Nevertheless the present solutions can be used to gain insight into the influence of the geometry of the growing particle, such as that the spherical particles grow faster than the cylindrical- and planar particles. The planar particles grow slowest. Further, a criterion for the existence of similarity solutions for growth of planar, cylindrical and spherical particles is given. This criterion coincides with the one of the existence of mass conserving solutions. Herewith, it follows that for multi-component particles the computed solutions are always mass conserving. These results are of course for the case that the Gibbs-Thomson effect has been disregarded. The paper should be considered in the spirit of the existing Zener nucleation models where an extension has been made to a vector Stefan problem for particle growth in a multi-component alloy. The case of dissolution of a planar particle can be tackled similarly. For the dissolution of spherical and cylindrical (needle-shaped) particles one can use approximate analytic solutions.

Further, a formalism has been developed for interface reactions in diffusional particle dissolution and growth for multi-component alloys, for which a numerical method has been presented to deal with the nonlinear problem. A Picard and Newton approach for the solution of the nonlinear problem were compared, where the Newton method was more efficient. As an initial guess for the equilibrium concentrations, the interface concentrations from the similarity solution are used. The interface reaction rate parameter has a large impact on the dissolution or growth kinetics.

## Acknowledgment

## References

1. F. S. Ham, Theory of diffusion-limited growth, *Journal of Physics and Chemistry in Solids*, **6**, pp. 335–351, 1958.

2. F. S. Ham, Stress-assisted precipitation on dislocations, *Journal of Applied Physics*, **30**(6), pp. 915–926, 1958.

3. C. Zener, Theory of growth of spherical precipitates from solid solution, *Journal of Applied Physics*, **20**, pp. 950–953, 1949.

4. M. J. Whelan, On the kinetics of particle dissolution, *Metals Science Journal*, **3**, pp. 95–97, 1969.

5. A. B. Tayler, The mathemtical formulation of stefan problems, in: *Moving boundary problems in heat flow and diffusion*, J. R. Ockendon, W. R. Hodgkins (Eds.), pp. 120–137, Oxford, 1975.

6. S. D. Howison, Similarity solutions to the stefan problem and the binary alloy problem, *IMA Journal of Applied Mathematics*, **40**, pp. 147–161, 1988.

7. H. B. Aaron, G. R. Kotler, Second phase dissolution, *Metallurgical Transactions*, **2**, pp. 1651–1656, 1971.

8. F. V. Nolfi jr., P. G. Shewmon, J. S. Foster, The dissolution and growth kinetics of spherical particles, *Transactions of the Metallurgical Society of AIME*, **245**, pp. 1427–1433, 1969.

9. J.-O. Andersson and J. Ågren, Models for numerical treatment of multicomponent diffusion in simple phases, *Journal of Applied Physics*, **72**(4), pp. 1350–1355, 1981.

10. J. Ågren, Numerical treatment of diffusional reactions in multi-component alloys, *Journal of Physics and Chemistry of Solids*, **43**(4), pp. 285–391, 1982.

11. J. Ågren, G. P. Vassilev, Computer simulations of cementite dissolution in austenite, *Materials Science and Engineering*, **64**, pp. 95–103, 1984.

12. D. E. Coates, Diffusion-controlled precipitate growth in ternary systems i, *Metallurgical Transactions*, **3**, pp. 1203–1212, 1972.

13. J. P. Bourne, C. Atkinson, R. C. Reed, Diffusion-controlled growth in ternary systems, *Metallurgical and Materials Transactions A*, **25A**, pp. 2683–2694, 1994.

14. K. Thornton, J. Ågren, P. W. Voorhees, Modelling the evolution of phase boundaries in solids at the meso- and nano-scales, *Acta Materialia*, **51**, pp. 5675–5710, 2003.

15. O. Reiso, N. Ryum, J. Strid, Melting and dissolution of secondary phase particles in AlMgSi-alloys, *Metallurgical Transactions A*, **24A**, pp. 2629–2641, 1993.

16. R. Hubert, Modelisation numerique de la croissance et de la dissolution des precipites dans l'acier, *ATB Metallurgie*, **34–35**, pp. 4–14, 1995.

17. J. M. Vitek, S. A. Vitek, S. A. David, Modelling of diffusion controlled phase transformation in ternary systems and application to the ferrite-austenite transformation in the Fe-Cr-Ni-system, *Metallurgical Transactions A*, **26A**, pp. 2007–2025, 1995.

18. I. Vusanovic, M. J. Krane, Microsegregation during solidification of Al-Cu-Mg alloys with varying composition, *International Communications in Heat and Mass Transfer*, **29**(3), pp. 1037–1046, 2002.

19. C. Atkinson, T. Akbay, R. C. Reed, Theory for reaustenization from ferrite-cementite mixtures in Fe-C-X steels, *Acta Metallurgica et Materialia*, **43**(5), pp. 2013–2031, 1995.

20. F. J. Vermolen, C. Vuik, S. van der Zwaag, Particle dissolution and cross-diffusion in multi-component alloys, *Materials Science and Engineering A*, **A347**, pp. 265–279, 2003.

21. F. J. Vermolen, C. Vuik, Solution of vector valued stefan problems with cross-diffusion, *Journal of Computational and Applied mathematics*, **176**(1), pp. 179–201, 2005.

22. J. Crank, *Free and moving boundary problems*, Clarendon Press, Oxford, 1984.

23. A. Segal, C. Vuik, F. J. Vermolen, A conserving discretisation for the free boundary in a two-dimensional stefan problem, *Journal of Computational Physics*, **141**, pp. 1–21, 1998.

24. W. D. Murray, F. Landis, Numerical and machine solutions of transient heat conduction problems involving freezing and melting, *Transactions ASME (C), Journal of Heat Transfer*, **245**, pp. 106–112, 1959.

25. S. Osher, J. A. Sethian, Fronts propagating with curvature-dependent speed, Algorithms based on hamilton-jacobi formulations, *Journal of Computational Physics*, **141**, pp. 12–49, 1988.

26. J. A. Sethian, *Level-Set methods and fast marching methods*, Cambridge University Press, New York, 1999.

27. S. Osher, R. Fedkiw, *Level-Set methods and dynamic implicit surfaces*, Springer-Verlag, New York, 2003.

28. S. Chen, B. Merriman, S. Osher, P. Smereka, A simple Level-Set method for solving Stefan problems, *Journal of Computational Physics*, **135**, pp. 8–29, 1997.

29. E. Javierre, C. Vuik, F. J. Vermolen, S. van der Zwaag, A comparison of numerical models for one-dimensional stefan problems, *Journal of Computational and Applied Mathematics*, **192**(2), pp. 445–459, 2006.

30. I. Kovačević, B. Šarler, Solution of a phase-field model for dissolution of primary particles, *Materials Science and Engineering A*, **413–414**, pp. 423–428, 2005.

31. F. J. Vermolen, E. Javierre, C. Vuik, L. Zhao, S. van der Zwaag, A three dimensional model for particle dissolution in binary alloys, *Journal of Computational Materials Science*, to appear.

32. E. Javierre, C. Vuik, F. J. Vermolen, A. Segal, A level set method for higher dimensional vector Stefan problems: computer simulations of particle dissolution in multi-component alloys, *Journal of Computational Physics*, to appear.

33. F. J. Vermolen, C. Vuik, E. Javierre, S. van der Zwaag, Review on some stefan problems for particle dissolution in solid state alloys, *Nonlinear Analysis: modelling and control*, **10**(3), pp. 257–292, 2005.

34. F. J. Vermolen, P. L. J. Zitha, J. Bruining, A model for a viscous preflush prior to gelation in a porous medium, *Computing and Visualization in Science*, **4**, pp. 205–212, 2002.

35. W. W. Mullins, R. F. Sekerka, Morphological instability of a particle growing by diffusion or heat flow, *Journal of Applied Physics*, **34**(2), pp. 323–329, 1963.

36. W. W. Mullins, R. F. Sekerka, Stability of planar interface during solidification of dilute binary alloy, *Journal of Applied Physics*, **35**(2), pp. 444–451, 1964.

37. J. Chadam, S. D. Howison, P. Ortoleva, Existence and stability for spherical crystals growing in a supersaturated solution, *IMA Journal of Applied Mathematics*, **39**, pp. 1–15, 1987.

38. F. J. Vermolen, C. Vuik, A vector valued Stefan problem from aluminium industry, *Nieuw Archief voor Wiskunde*, **17**, pp. 205–217, 1999.

39. O. R. Myhr, Ø. Grong, Modelling of non-isothermal transformations in alloys containing a particle distribution, *Acta Materialia*, **48**, pp. 1605–1615, 2000.

40. F. J. Vermolen, C. Vuik, A mathematical model for the dissolution of particles in multi-component alloys, *Journal of Computational and Applied Mathematics*, **126**, pp. 233–254, 2001.

41. F. S. Ham, Diffusion-limited growth of precipitate particles, *Journal of Applied Physics*, **30**(10), pp. 1518–1525, 1959.

42. F. J. Vermolen, C. Vuik, S. van der Zwaag, Cross-diffusion controlled particle dissolution in metallic alloys, *Computing and Visualization in Science*, **8**, pp. 27–33, 2005.